

Prediction of a potential drug target based on protein druggability for thyroid cancer

YiFei Yang (✉ suncancer2020@gmail.com)

the first people's hospital of yuhang <https://orcid.org/0000-0002-1659-6473>

Bin Yu

the first people's hospital of yuhang

Xiu-Xia Zhang

the first people's hospital of yuhang

Yun-Hua Zhu

the first people's hospital of yuhang

Primary research

Keywords: thyroid cancer, WGCNA, drug target, druggability, drug repositioning , informatics

Posted Date: May 27th, 2020

DOI: <https://doi.org/10.21203/rs.3.rs-30875/v1>

License: © ⓘ This work is licensed under a Creative Commons Attribution 4.0 International License.

[Read Full License](#)

1 Prediction of a potential drug target based on 2 protein druggability for thyroid cancer

3 Yi-Fei Yang^{1*}, Bin Yu², Xiu-Xia Zhang², Yun-Hua Zhu²

4 *Correspondence: suncancer2020@gmail.com

5 1. Department of Thyroid and Breast Surgery, The First People' s Hospital of

6 Yuhang, Hangzhou, Zhejiang, P.R. China.

7 2. Department of Thyroid and Breast Surgery, The First People' s Hospital of

8 Yuhang, Hangzhou, Zhejiang, P.R. China.

9 Abstract

10 **Background:** Thyroid cancer is a common endocrine malignancy; however, its
11 treatment is still surgical. With the development and application of targeted
12 therapy in cancer treatment, there are great development prospects in researching
13 targeted drugs for thyroid cancer.

14 **Methods:** Differentially expressed mRNAs between thyroid cancerous tissue and
15 normal thyroid tissues were screened from The Cancer Genome Atlas (TCGA)
16 database. Using weighted gene coexpression network analysis (WGCNA) to build
17 co-expression modules and combined with differentially methylated gene (DMG)
18 analysis. The druggability was analyzed by PockDrug-Server. Due to drug
19 repositioning to seek targeted drugs to treat thyroid cancer we constructed a
20 protein-protein interaction (PPI) network, and screened out a drug target of thyroid
21 cancer. Gene Ontology (GO) and Kyoto Encyclopedia of Genes and Genomes
22 pathway (KEGG) were used to analysis the protein enrichment of PPI network.

23 **Results:** In the present study, the red module was significantly correlated with
24 thyroid cancer. With DMG analysis, we screened out three genes: *HEY2*, *TNIK* and
25 *LRP4*. These three genes were hypomethylation in tumors. The druggability based
26 on PockDrug-Server predicted that only TNIK had protein pocket druggability. With
27 PPI model for TNIK, there were ten genes interacted with TNIK. These genes were
28 enriched in the MAPK and Wnt pathways, which are correlated with tumor
29 proliferation, differentiation, and development. Upon searching for drugs against
30 these 10 genes in Drugbank, it was determined that the targeted drug Binimetinib
31 which is MEK1/2 inhibition. Therefore, we hypothesized that Binimetinib can be
32 used as a targeted drug and TNIK can be regard as drug target for thyroid cancer
33 therapy.

34 **Conclusion:** Our research provides a bioinformatics method for screening drugs
35 target and provides a theoretical basis for targeted therapy for thyroid cancer.

36 **Key words:** thyroid cancer, WGCNA, drug target, druggability, drug repositioning,
37 informatics

38 **Background**

39 Thyroid cancer (TC) is a common type of endocrine malignancy that primarily consists of
40 papillary, follicular, medullary and anaplastic carcinomas. Thyroid cancer is one of the fastest
41 growing cancers. In the past few years, the rate of thyroid cancer incidence has increased
42 observably, with 56,460 new diagnoses of thyroid cancer in the USA, at an approximate 5%
43 growth rate [1]. The morbidity has increased from ~10/1,000,000 to 30-40/1,000,000 in China [2].
44 Although the major treatments, such as thyroidectomy, radioiodine therapy and

45 thyroid-stimulating hormone inhibition therapy, have achieved great advancements, the targeted
46 drugs for thyroid cancer are unsatisfactory [3]. Therefore, it is essential to explore novel drug
47 targets for treatment.

48 Epigenetic changes are regarded as significant contributors to tumor progression [4]. DNA
49 methylation is one of the most important epigenetic modifications, as it does not alter the DNA
50 sequence but changes gene expression. Alterations of its status can lead to the development and
51 progression of various cancers. For example, *BRCA1* is methylated and associated with the
52 inactivation of gene expression in breast cancers [5,6]; glutathione S-transferase methylation has a
53 strong correlation with the mortality of prostate cancer patients [7]. Methylation can be used as a
54 prognostic biomarker and therapeutic target for cancer species and has great potential in cancer
55 therapy [8–10]. Roy and Kandimalla et al. researched lymph node metastasis and built a
56 comprehensive methylation signature for predicting the prognosis of esophageal squamous cell
57 carcinoma patients [11]. Some studies also indicate that methylation serves as cancer therapeutic
58 target. For instance, Hegi et al determined that glioblastomas with *MGMT* methylation showed
59 sensitivity to temozolomide (TMZ) [12]. Fujii et al. found that *HSD17B4* methylation showed
60 sensitivity to trastuzumab combined with chemotherapy in HER2-positive breast cancer patients
61 [13]. The therapy for thyroid cancer is closely associated with aberrant DNA methylation. In
62 recent years, more and more thyroid cancer therapy management in patients is shifting toward
63 personalized medicine to avoid the overdiagnosis and overtreatment of tumors [14]. However,
64 there have been few studies on the abnormal methylation of thyroid cancer patients.

65 Drug research and design is a complex and a lengthy period that requires a lot of investment.

66 Shortening the time and reducing the cost for drug development becomes a tricky problem. Drug

67 repositioning is to confirm a new use of the drug which have approved [15]. This method greatly
68 reduces the time and cost for people to develop drugs. Protein–protein interaction (PPI) network is
69 one of methods to identify drug repositioning. Constructing PPIs for drug targets or differentially
70 expressed genes, and determine the possible drugs for diseases through their interactions with
71 known drug targets or proteins with indirect effects [16]. In recent years, more and more academic
72 researchers are interested in drug repositioning. Wang et al. detected 3 drug targets and 15
73 candidate drugs by WGCNA and PPI for treating melanoma [17]. Islam et al. identified 238 gene
74 signatures as therapeutic targets from PPI analysis and 37 novel drugs as potential anticancer
75 drugs for low-grade glioma [18]. We used druggability analyze and PPI to provide novel drug
76 target and agents for treatment and improve the survival rate of thyroid cancer patients.

77 In the current study, we identified three hub genes of thyroid cancer by constructing a
78 coexpression network of WGCNA combined with differential methylation analysis, employing
79 PockDrug druggability and protein-protein interaction network analyses to find drug target.
80 Furthermore, our study might offer new insight and therapeutic options for the treatment of
81 thyroid cancer.

82 **Methods**

83 **Data and Sources**

84 RNA-seq and DNA methylation data of thyroid cancer tissue and corresponding normal tissue
85 were downloaded from The Cancer Genome Atlas (TCGA, <https://cancergenome.nih.gov/>). We
86 selected the top 5000 mRNAs for 568 samples of differentially expressed genes (DEGs) for a
87 Weighted Gene Co-Expression Network Analysis (WGCNA). The mRNA sequencing data were
88 normalized by the edgeR package in R language and CMP to screen out the expression of more

89 than one in three samples [19]. The cut-off criteria of adjusted $|\log_2 \text{fold change (FC)}| > 1$ and
90 $\text{FDR} < 0.05$ were considered to be statistically significant.

91 **Weighted Gene Co-Expression Network Analysis (WGCNA)**

92 The “WGCNA” R package was used to construct a coexpression network for the screened out
93 genes [20]. First, the DEGs and the Pearson correlations were used to confirm the most correlated
94 genes and to exclude weakly correlated genes. We calculated the soft thresholding power (β) by
95 network topology analysis and converted the adjacency to the topological overlap matrix (TOM)
96 [21]. Second, a gene dendrogram was constructed by hierarchical clustering. We used a dynamic
97 tree-cut algorithm to separate branches of a gene dendrogram from modules of coexpressed genes
98 into different colors [22]. The $\text{deepsplit} = 2$ and $\text{minimal module size} = 30$. Third, we estimated
99 the similarity of modules and merged the highly coexpression genes. Setting of 0.25 as the
100 threshold was chosen as the dissimilarity between the modules and the merged highly coexpressed
101 modules. Then, the module-traits relationship (MTR) was constructed by measuring the relevance
102 between the module eigengenes and thyroid cancer tissues [22]. For the correlations and to
103 calculate the gene significance and module membership, $\text{p-value} < 0.05$.

104 **Differentially Methylated Genes Analysis**

105 DNA methylation data were based on the annotations by the TCGA. The differentially methylated
106 genes between thyroid cancer tissues and normal adjacent tissues were analyzed with the “minfi”
107 package in R software. First, we conducted a t-test and screened out the data for $\text{FDR} < 0.05$. Then,
108 to calculate the different beta-values of the screened data, we considered the beta-value
109 differences greater than 0.3 as hypermethylation and less than 0.3 as hypomethylation between
110 thyroid cancer tissues and normal adjacent tissues.

111 **PockDrug druggability and Protein and Protein Interaction Analyses**

112 PockDrug (<http://pockdrug.rpbs.univ-paris-diderot.fr/>) is a robust, pocket druggability prediction
113 server with references to pocket boundary uncertainties and can queried for a protein or a set of
114 proteins [23]. Therefore, according to PockDrug, we predicted the druggability of the genes in
115 both the hub module and the DMGs. A druggability probability greater than 0.5 was considered a
116 druggable pocket.

117 Due to drug repositioning, we identified the interaction proteins regarding the druggability of
118 TNIK. To analyze proteins using the Search Tool for the Retrieval of Interacting Genes (STRING)
119 database (<http://string-db.org/>), which calculates protein–protein association data for a great
120 amount of organisms and can uncover direct (physical) and indirect (functional) relationships to
121 construct a PPI network for TNIK, with a minimum required interaction score of 0.7. The data
122 were visualized by Cytoscape v3.3.0 software to construct the network [24–26].

123 **Functional Enrichment Analysis**

124 Functional enrichment analysis was performed using the Database for Annotation, Visualization,
125 and Integrated Discovery (DAVID) v.6.8 (<https://david.ncifcrf.gov/>), a web-accessible program
126 that integrates functional genomic annotations by intuitive graphical summaries [27], annotates
127 genes and carries out Gene Ontology (GO) analysis, including biological process (BP), molecular
128 function (MF) and cellular component (CC) [28]. Kyoto Encyclopedia of Genes and Genomes
129 (KEGG, version 90.0; www.kegg.jp) is one of the most common online resources for interpreting
130 biological systems from molecular level data [29]. Thus, DAVID was used to annotate genes in
131 PPI, and GO and KEGG term enrichments were analyzed. $P < 0.05$ was regarded as a statistically
132 significant difference.

133 **Results**

134 **WCGNA analysis and module significance calculation**

135 The top 5000 DEGs of RNA-seq data for thyroid cancer were from TCGA, which was used to
136 construct the coexpression network. We chose the best value for the scale independence property
137 of the network when the soft threshold power was set at 3 and the scale-free R² reached 0.9 to
138 construct the coexpression module (Fig. 1). A total of 10 modules were identified, and these gene
139 clusters were displayed as a dendrogram and shown in different colors in Fig. 2a. To smoke out
140 the connections between genes in each module and thyroid cancer samples, the correlations of the
141 module eigengenes were correlated with cancer tissues and normal tissues, as shown in Fig. 2b.
142 The eigengene dendrogram and adjacency heatmap were provided in Fig. 2c. The red module ($r =$
143 0.51 ; $p = 3e-38$) and the blue module ($r = 0.51$; $p = 5e-39$) showed the greatest positive
144 associations and the green module ($r = -0.53$; $p = 2e-24$) showed the greatest negative associations
145 with thyroid tumorigenesis. According to the correlation between module membership and gene
146 significance (Fig. 2d), the red module had a high correlation ($cor = 0.73$; $p = 9.7e-26$), and this
147 module was selected for further analysis.

148 **DMGs in the Red Module**

149 We used methylation data from TCGA thyroid cancer. Methylated genes identified by t-test and
150 $FDR < 0.05$ were regarded as discriminative methylation. We found 445 genes identified as DMGs.
151 Meanwhile, intersection analysis between DMGs and genes in the red module screened three
152 genes, *HEY2*, *TNIK* and *LRP4* (Fig. 3a), as candidates to be further analyzed for druggability. The
153 heatmap of these three genes is shown in Fig. 3b. These three genes were hypomethylated in
154 thyroid cancer tissues.

155 **Pocket Druggability prediction of HEY2, TNIK, and LRP4 proteins**

156 Druggability is the capacity for a protein to bind drug-like molecules with a high affinity [30].
157 Therefore, it is necessary to assess druggability as the first step of drug discovery. Study of the
158 protein pocket druggability behavior is a key step in the target identification stage of drug
159 discovery. In our study, we used the PockDrug-Server to predict the pocket druggability of HEY2,
160 TNIK and LRP4 proteins. Following our prediction, only TNIK, which consists of 538 residues,
161 had eight protein pockets (P0-P7, respectively) (Fig. 4). The protein pockets with an average
162 druggability probability greater than 0.5 were considered as druggable pockets. Table 1 shows the
163 parameters of the eight protein pockets, and the result indicated that P0 (0.9, $p = 0.01$), P2 (0.82, p
164 $= 0.05$), P3 (0.86, $p = 0.0$) and P6 (0.92, $p = 0.02$) had the highest druggability probability.
165 Accordingly, we considered TNIK as a possible drug target for thyroid cancer.

166 **PPI of TNIK and targeted drug analysis**

167 To seek out thyroid cancer-targeted drugs, we identified Fostamatinib as a targeted drug of TNIK
168 through Drugbank (<https://www.drugbank.ca/>). But Fostamatinib has been confirmed to have
169 effects on rheumatoid arthritis and immune thrombocytopenic purpura (ITP). Due to drug
170 repositioning, we constructed a network of PPI for TNIK using Cytoscape, which consisted of 11
171 nodes and 39 edges from the STRING database. Ten proteins interacted with TNIK (Fig. 5). To
172 determine the biological functions of genes in the PPI, we performed GO and KEGG pathway
173 enrichment analysis. The genes were enriched in positive regulation of protein phosphorylation,
174 positive regulation of MAPK cascade, beta-catenin-TCF7L2 complex, kinase binding and protein
175 phosphatase binding (Fig. 6). According to KEGG analysis, there was enrichment in the MAPK
176 signaling pathway, the TNF signaling pathway and amyotrophic lateral sclerosis (ALS), among

177 other pathways (Table 2). Drugbank found a targeted drug for these 10 proteins, Binimetinib,
178 which targeted MAP3K1. Thereby, Binimetinib may serve as targeted drug in future therapy of
179 thyroid cancer.

180 **Discussion**

181 Thyroid cancer is a common endocrine malignancy; however, there are few targeted therapeutic
182 drugs available. In this study, we constructed a coexpression network based on mRNA profiles in
183 thyroid cancer and then used the PockDrug-Server in combination with PPI analysis to identify
184 genes that could be targeted to thyroid cancer for treatment. A total of 10 coexpression modules
185 were structured based on the top 5000 DEGs between thyroid cancer and normal samples by
186 WGCNA, and the red module was determined to have the greatest correlation with thyroid cancer.
187 Based on interactions with the red module and DMGs, we screened out three hub genes, *HEY2*,
188 *TNIK* and *LRP4*. Our heatmap results showed that these three genes were hypomethylated in
189 neoplasm tissue (Figure 3B). DNA hypomethylation can cause normally silenced genes to be
190 harmfully expressed, leading to genomic instability [31,32]. DNA hypomethylation is associated
191 with neoplastic progression or postoperative recurrence of disease [33,34]. Therefore DNA
192 hypomethylation can serve as a cancer biomarker. It is estimated that *HEY2*, *TNIK* and *LRP4* play
193 important physiologic roles in the occurrence of thyroid cancer. *HEY2* has been confirmed that
194 correlated with the proliferation of papillary thyroid cancer [35]. *LRP4* has been validated as
195 anovel oncogene in papillary thyroid carcinoma [36].

196 Protein pocket druggability is a tool for predicting the high affinity of a protein pocket's ability to
197 bind drug-like molecules and is a major mark in the identification phase of drug target discovery
198 [37]. To confirm whether *HEY2*, *TNIK*, or *LRP4* have druggable protein pockets, we predicted

199 them using PockDrug-Server. PockDrug-Server is a new bioinformatics tool for efficiently
200 measuring the druggability of holo- and apoprotein pockets. Compared with other druggability
201 models, it can effectively distinguish the degree of the protein pocket's druggability through a
202 unique bioinformatics algorithm [38]. A large number of studies have shown that
203 PockDrug-Server is an optimal predictive model of druggability for apoprotein pockets.
204 Muhammad Hamza et al. ascertained P53 Ser121 and Val122 mutations as drug targets using
205 PockDrug-Server [39]. Trigueiro-Louro et al. used PockDrug-Server to predict the druggable sites
206 in the effector domain of NS1 protein and then identified 3 druggable pockets and 8 new potential
207 hot spot residues in the NS1 protein [40]. In this study, we used PockDrug-Server to predict
208 druggable pockets of HEY2, TNIK and LRP4. It showed that only TNIK had protein pockets and
209 indicated that it had 4 druggable protein pockets (Table 1). Consequently, we hypothesized that
210 TNIK may be a drug target in thyroid cancer.

211 TNIK (Traf2- and Nck-interacting kinase) is a member of the Ste20 superfamily and has
212 previously been shown to regulate a variety of cellular processes, including apoptosis,
213 morphogenesis and the cytoskeletal regulation of cell shape and motility [41]. Abnormal
214 expression or mutation of TNIK can cause cells to become cancerous. Studies have shown that
215 high expression of TNIK may accelerate tumor progression and invasion by activating the Wnt
216 signaling pathways in terminal colorectal cancer patients [42]. Shitashige et al. suggested that
217 TNIK as a feasible drug target for colorectal cancer because it can affect the proliferation of
218 colorectal cancer cells [43]. Moreover, TNIK is also a novel therapeutic target in gastric cancer, as
219 its amplification could activate the PI3K/Akt pathway to promote tumorigenesis [44]. In the
220 present study, we considered that TNIK might promote thyroid cancer development by

221 hypomethylation and could influence the treatment of thyroid cancer.

222 We structured the PPI of TNIK and found that a total of 10 genes were related to TNIK.

223 Enrichment analysis revealed that they were primarily enriched in intracellular signal transduction,

224 positive regulation of the MAPK cascade and the Wnt signaling pathway. KEGG pathway

225 enrichment indicated that most genes were concentrated in the Mitogen-activated protein kinases

226 (MAPKs) signaling pathway and the Tumor necrosis factor (TNF) signaling pathway. The MAPKs

227 and TNF signaling pathways are common pathogenic signaling networks that influence cellular

228 proliferation, differentiation, development, inflammatory responses and apoptosis in tumors

229 [45,46]. There are some small inhibitors can suppress MAPKs pathway effectors to affect the

230 growth of thyroid cancer cells. Of these 10 genes, TNF, TNFRSF1A, TRAF2 and TRADD are the

231 key effector molecules in the TNF signaling pathway [47–50], of which TRAF2 can activate the

232 MAPK pathway, and TCF7L2 with CTNNB1 can activate WNT/ β -catenin signaling [51,52]. The

233 expression of CTNNB1 is related to thyroid tumor aggressiveness [53]. MAP3K1, MAP2K6,

234 MAP2K3 and MAP2K5 are the effectors of the MAPKs pathway. MAP3K1 is a member of the

235 MAP3K family and the STE superfamily and plays a vital part in the MAPKs pathway [46,54].

236 MAP3K1 and TNIK are important kinases in the activation of Wnt/ β -catenin signaling in cancer

237 cell lines [55]. Research has shown that MAP3K1 promotes Wnt/ β -catenin signaling, and TNIK

238 has been found to be primarily involved in β -catenin-dependent transcriptional activation in colon

239 cancer cell lines [56,57]. Based on these interactions with TNIK, we looked up the targeted drugs

240 on Drugbank and found that only MAP3K1 has a targeted drug, Binimetinib, which is a potent and

241 selective oral mitogen-activated protein kinase 1/2 (MEK 1/2) inhibitor.

242 In recent years, with the growth of targeted therapy, it has become a most attractive strategy of

243 cancer therapy. However, surgery is still the main method for thyroid cancer treatment, as less is
244 known about targeted therapies for thyroid cancer. However, drug research is a complex, long
245 process and requires a great deal of investment. Drugs usually have a specific effect on one or
246 more target proteins [58]. Drug repositioning is a good selection step to overcome the limitations
247 of traditional methods. Drug repositioning can find novel uses for existing drugs through PPI to
248 reduce the costs and risks of drug development [59]. We predicted that Binimetinib may be a
249 potential targeted drug for thyroid cancer based on the PPI network of TNIK. The FDA (Food and
250 Drug Administration) approved the combination of Binimetinib and Encorafenib for patients with
251 unresectable or metastatic melanoma with $BRAF^{V600E}$ or $^{-V600K}$ mutation on June 27, 2018. There
252 has also been new clinical research on Binimetinib in the treatment of thyroid cancer with
253 $BRAF^{V600E}$ mutation (NCT04061980). Therefore, Binimetinib is likely to have potential effects in
254 treating thyroid cancer.

255 Due to the restriction of information for PPI collection regarding detailed interaction dynamics,
256 the prediction results are not comprehensive. Binimetinib for thyroid cancer remains on clinical
257 trial; therefore, its efficacy and safety still require experimentation for verification. Our predicted
258 results provide a theoretical basis for future targeted therapy of thyroid cancer.

259 **Conclusions**

260 In conclusion, using WGCNA, PockDrug druggability and PPI analyses for thyroid cancer-related
261 genes, we revealed that TNIK could serve as a potential drug target correlated with the treatment
262 of thyroid cancer. Further studies that provide a method to screen the targeted gene, which has
263 druggability and to explore the potential drug target on thyroid cancer are imperative. We hope
264 these findings will contribute to the research on new targeted therapeutic drugs for thyroid cancer.

265 **Abbreviations**

266 TCGA: The Cancer Genome Atlas; WGCNA: Weighted Gene Coexpression Network Analysis;
267 DEGs: Differentially Expressed Genes; DMGs: Differentially Methylated Genes; PPI:
268 Protein-Protein Interaction; GO: Gene Ontology; KEGG: Kyoto Encyclopedia of Genes and
269 Genomes pathway; MAPK: Mitogen-activated protein kinases; MEK1/2: Mitogen-activated
270 protein kinase 1/2.

271 **Acknowledgements**

272 Not applicable.

273 **Authors' contributions**

274 YFY and BY conceived and designed the study; BY, XXZ and YHZ carried out data collection
275 and performed data analysis; YFY wrote the paper; BY, XXZ and YHZ dited the manuscript and
276 provided critical comments. All authors read and approved the final manuscript.

277 **Funding**

278 Not applicable.

279 **Availability of data and materials**

280 The datasets generated and during the current study are available in the TCGA repository,
281 <https://cancergenome.nih.gov/>.

282 **Ethics approval and consent to participate**

283 Not applicable.

284 **Consent for publication**

285 Not applicable.

286 **Competing interests**

287 The authors declare that they have no competing interests.

288 **Author details**

289 ^{1,2} Department of Thyroid and Breast Surgery, The First People's Hospital of Yuhang, Hangzhou
290 311100, Zhejiang, P.R. China.

291 **Reference**

- 292 1. Siegel RL, Miller KD, Jemal A. Cancer statistics, 2016. *CA Cancer J Clin.* 2016;66:7–30.
- 293 2. Li JY, Shi J, Sang JF, Yao YZ, Wang XC, Su L. Role of survivin in the pathogenesis of
294 papillary thyroid carcinoma. *Genet Mol Res.* 2015;14:15102–11.
- 295 3. Lundgren CI, Hall P, Dickman PW, Zedenius J. Clinically significant prognostic factors
296 for differentiated thyroid carcinoma: A population-based, nested case-control study.
297 *Cancer.* 2006;106:524–31.
- 298 4. Jones PA, Baylin SB. The Epigenomics of Cancer. *Cell.* 2007;128:683–92.
- 299 5. Esteller M. Promoter Hypermethylation and BRCA1 Inactivation in Sporadic Breast
300 and Ovarian Tumors. *J Natl Cancer Inst.* 2000;92:564–9.
- 301 6. Rice JC. Transcriptional repression of BRCA1 by aberrant cytosine methylation,
302 histone hypoacetylation and chromatin condensation of the BRCA1 promoter. *Nucleic*
303 *Acids Res.* 2000;28:3233–9.
- 304 7. Richiardi L, Fiano V, Grasso C, Zugna D, Delsedime L, Gillio-Tos A, et al. Methylation of
305 APC and GSTP1 in Non-Neoplastic Tissue Adjacent to Prostate Tumour and Mortality
306 from Prostate Cancer. *PLoS One.* 2013;8:1–7.
- 307 8. Tang J, Xiong Y, Zhou HH, Chen XP. DNA methylation and personalized medicine. *J*
308 *Clin Pharm Ther.* 2014;39:621–7.

- 309 9. Lv JF, Hu L, Zhuo W, Zhang CM, Zhou HH, Fan L. Epigenetic alternations and cancer
310 chemotherapy response. *Cancer Chemother Pharmacol*. Springer Berlin Heidelberg;
311 2016;77:673–84.
- 312 10. Xing MM. Minireview: Gene methylation in thyroid tumorigenesis. *Endocrinology*.
313 2007;148:948–53.
- 314 11. Roy R, Kandimalla R, Sonohara F, Koike M, Kodera Y, Takahashi N, et al. A
315 comprehensive methylation signature identifies lymph node metastasis in esophageal
316 squamous cell carcinoma. *Int J Cancer*. 2019;144:1160–9.
- 317 12. Hegi ME, Diserens AC, Gorlia T, Hamou MF, De Tribolet N, Weller M, et al. MGMT
318 gene silencing and benefit from temozolomide in glioblastoma. *N Engl J Med*.
319 2005;352:997–1003.
- 320 13. Fujii S, Yamashita S, Yamaguchi T, Takahashi M, Hozumi Y, Ushijima T, et al.
321 Pathological complete response of HER2-positive breast cancer to trastuzumab and
322 chemotherapy can be predicted by HSD17B4 methylation. *Oncotarget*. 2017;8:19039–
323 48.
- 324 14. Dralle H, MacHens A, Basa J, Fatourechhi V, Franceschi S, Hay ID, et al. Follicular
325 cell-derived thyroid cancer. *Nat Rev Dis Prim* [Internet]. Macmillan Publishers Limited;
326 2015;1:1–19. Available from: <http://dx.doi.org/10.1038/nrdp.2015.77>
- 327 15. Naylor S, Kauppi DM, Schonfeld JM. Therapeutic drug repurposing, repositioning
328 and rescue: Part II: Business review. *Drug Discov World*. 2015;16:57–72.
- 329 16. Azuaje F. Drug interaction networks: An introduction to translational and clinical
330 applications. *Cardiovasc Res*. 2013;97:631–41.

331 17. Wang L, Wei CY, Xu YY, Deng XY, Wang Q, Ying JH, et al. Prognostic genes of
332 melanoma identified by weighted gene co-expression network analysis and drug
333 repositioning using a network-based method. *Oncol Lett.* 2019;18:6066–78.

334 18. Islam T, Rahman MR, Shuvo MAH, Shahjaman M, Islam MR, Karim MR. Drug
335 repositioning and biomarkers in low-grade glioma via bioinformatics approach.
336 *Informatics Med Unlocked* [Internet]. Elsevier Ltd; 2019;17:100250. Available from:
337 <https://doi.org/10.1016/j.imu.2019.100250>

338 19. Robinson MD, McCarthy DJ, Smyth GK. edgeR: A Bioconductor package for
339 differential expression analysis of digital gene expression data. *Bioinformatics.*
340 2009;26:139–40.

341 20. Horvath S, Zhang B, Carlson M, Lu K V., Zhu S, Felciano RM, et al. Analysis of
342 oncogenic signaling networks in glioblastoma identifies ASPM as a molecular target.
343 *Proc Natl Acad Sci U S A.* 2006;103:17402–7.

344 21. Botía JA, Vandrovcova J, Forabosco P, Guelfi S, D’ Sa K, Hardy J, et al. An additional
345 k-means clustering step improves the biological features of WGCNA gene
346 co-expression networks. *BMC Syst Biol. BMC Systems Biology;* 2017;11:1–16.

347 22. Langfelder P, Horvath S. WGCNA: An R package for weighted correlation network
348 analysis. *BMC Bioinformatics.* 2008;9.

349 23. Hussein HA, Borrel A, Geneix C, Petitjean M, Regad L, Camproux AC.
350 PockDrug-Server: A new web server for predicting pocket druggability on holo and apo
351 proteins. *Nucleic Acids Res.* 2015;43:W436–42.

352 24. Szklarczyk D, Morris JH, Cook H, Kuhn M, Wyder S, Simonovic M, et al. The STRING

353 database in 2017: Quality-controlled protein-protein association networks, made
354 broadly accessible. *Nucleic Acids Res.* 2017;45:D362–8.

355 25. Szklarczyk D, Franceschini A, Wyder S, Forslund K, Heller D, Huerta-Cepas J, et al.
356 STRING v10: Protein-protein interaction networks, integrated over the tree of life.
357 *Nucleic Acids Res.* 2015;43:D447–52.

358 26. Su G, Morris JH, Demchak B, Bader GD. Biological Network Exploration with
359 Cytoscape 3. *Curr Protoc Bioinforma.* 2014;2014:8.13.1-8.13.24.

360 27. Dennis G, Sherman BT, Hosack DA, Yang J, Gao W, Lane HC, et al. DAVID: Database
361 for Annotation, Visualization, and Integrated Discovery. *Genome Biol.* 2003;4:2003.

362 28. Huang DW, Sherman BT, Tan Q, Collins JR, Alvord WG, Roayaei J, et al. The DAVID
363 Gene Functional Classification Tool: A novel biological module-centric algorithm to
364 functionally analyze large gene lists. *Genome Biol.* 2007;8.

365 29. Kanehisa M, Subramaniam. The KEGG database. *Novartis Found Symp.*
366 2002;247:91–103.

367 30. Hopkins AL, Groom CR. Opinion: The druggable genome. *Nat Rev Drug Discov.*
368 2002;1:727–30.

369 31. Eze OP, Starker LF, Carling T. The role of epigenetic alterations in papillary thyroid
370 carcinogenesis. *J Thyroid Res.* 2011;2011.

371 32. Moore LE, Pfeiffer RM, Poscablo C, Real FX, Kogevinas M, Silverman D, et al.
372 Genomic DNA hypomethylation as a biomarker for bladder cancer susceptibility in the
373 Spanish Bladder Cancer Study: a case-control study. *Lancet Oncol.* 2008;9:359–66.

374 33. Pulukuri SMK, Estes N, Patel J, Rao JS. Demethylation-linked activation of urokinase

375 plasminogen activator is involved in progression of prostate cancer. *Cancer Res.*
376 2007;67:930–9.

377 34. Itano O, Ueda M, Kikuchi K, Hashimoto O, Hayatsu S, Kawaguchi M, et al. Correlation
378 of postoperative recurrence in hepatocellular carcinoma with demethylation of
379 repetitive sequences. *Oncogene.* 2002;21:789–97.

380 35. Wang DP, Tang XZ, Liang QK, Zeng XJ, Yang JB, Xu J. microRNA-599 promotes
381 apoptosis and represses proliferation and epithelial-mesenchymal transition of
382 papillary thyroid carcinoma cells via downregulation of Hey2-dependent Notch
383 signaling pathway. *J Cell Physiol.* 2020;235:2492–505.

384 36. Zhou X, Xia E, Bhandari A, Zheng C, Xiang J, Guan Y, et al. LRP4 promotes
385 proliferation, migration, and invasion in papillary thyroid cancer. *Biochem Biophys Res*
386 *Commun* [Internet]. Elsevier Ltd; 2018;503:257–63. Available from:
387 <https://doi.org/10.1016/j.bbrc.2018.06.012>

388 37. Abi Hussein H, Geneix C, Petitjean M, Borrel A, Flatters D, Camproux AC. Global
389 vision of druggability issues: applications and perspectives. *Drug Discov Today*
390 [Internet]. Elsevier Ltd; 2017;22:404–15. Available from:
391 <http://dx.doi.org/10.1016/j.drudis.2016.11.021>

392 38. Borrel A, Regad L, Xhaard H, Petitjean M, Camproux AC. PockDrug: A model for
393 predicting pocket druggability that overcomes pocket estimation uncertainties. *J Chem*
394 *Inf Model.* 2015;55:882–95.

395 39. Hamza M, Mahmood A, Khan S, Rizwan M, Munir A. Design and Synthesis of Novel
396 Inhibitor against Ser121 and Val122 Mutations in P53 Cancer Gene. *Adv Pharmacol*

397 Pharm. 2019;7:63–70.

398 40. Trigueiro-Louro JM, Correia V, Santos LA, Guedes RC, Brito RMM,
399 Rebelo-de-Andrade H. To hit or not to hit: Large-scale sequence analysis and structure
400 characterization of influenza A NS1 unlocks new antiviral target potential. *Virology*
401 [Internet]. Elsevier Inc.; 2019;535:297–307. Available from:
402 <https://doi.org/10.1016/j.virol.2019.04.009>

403 41. Dan I, Watanabe NM, Kusumi A. The Ste20 group kinases as regulators of MAP
404 kinase cascades. *Trends Cell Biol.* 2001;11:220–30.

405 42. Takahashi H, Ishikawa T, Ishiguro M, Okazaki S, Mogushi K, Kobayashi H, et al.
406 Prognostic significance of Traf2- and Nck- interacting kinase (TNIK) in colorectal cancer.
407 *BMC Cancer* [Internet]. *BMC Cancer*; 2015;15:1–10. Available from:
408 <http://dx.doi.org/10.1186/s12885-015-1783-y>

409 43. Satow R, Shitashige M, Jigami T, Honda K, Ono M, Hirohashi S, et al. Traf2- and
410 Nck-interacting kinase is essential for canonical Wnt signaling in *Xenopus* axis
411 formation. *J Biol Chem.* 2010;285:26289–94.

412 44. Yu DH, Zhang X, Wang H, Zhang L, Chen H, Hu M, et al. Erratum: The essential role
413 of TNIK gene amplification in gastric cancer growth (*Oncogenesis* (2014) 3 (e89)
414 DOI:10.1038/oncsis.2014.2). *Oncogenesis.* 2014;3:9024.

415 45. Tracey KJ, Cerami A. Tumor necrosis factor, other cytokines and disease. *Annu Rev*
416 *Cell Biol.* 1993;9:317–43.

417 46. Uhlik MT, Abell AN, Cuevas BD, Nakamura K, Johnson GL. Wiring diagrams of MAPK
418 regulation by MEKK1, 2, and 3. *Biochem Cell Biol.* 2004;82:658–63.

419 47. Egusquiaguirre SP, Yeh JE, Walker SR, Liu S, Frank DA. The STAT3 Target Gene
420 TNFRSF1A Modulates the NF- κ B Pathway in Breast Cancer Cells. *Neoplasia* (United
421 States) [Internet]. The Authors; 2018;20:489–98. Available from:
422 <https://doi.org/10.1016/j.neo.2018.03.004>

423 48. Liu ZG. Molecular mechanism of TNF signaling and beyond. *Cell Res*. 2005;15:24–7.

424 49. Hsu H, Xiong J, Goeddel D V. The TNF receptor 1-associated protein TRADD signals
425 cell death and NF- κ B activation. *Cell*. 1995;81:495–504.

426 50. Wang CY, Mayo MW, Baldwin AS. TNF- and cancer therapy-induced apoptosis:
427 Potentiation by inhibition of NF- κ B. *Science* (80-). 1996;274:784–7.

428 51. Burwinkel B, Shanmugam KS, Hemminki K, Meindl A, Schmutzler RK, Sutter C, et al.
429 Transcription factor 7-like 2 (TCF7L2) variant is associated with familial breast cancer
430 risk: A case-control study. *BMC Cancer*. 2006;6:7–10.

431 52. Xing M. Molecular pathogenesis and mechanisms of thyroid cancer. *Nat Rev Cancer*
432 [Internet]. Nature Publishing Group; 2013;13:184–99. Available from:
433 <http://dx.doi.org/10.1038/nrc3431>

434 53. Garcia-Rostan G, Camp RL, Herrero A, Carcangiu ML, Rimm DL, Tallini G. β -catenin
435 dysregulation in thyroid neoplasms: Down-regulation, aberrant nuclear expression, and
436 CTNNB1 exon 3 mutations are markers for aggressive tumor phenotypes and poor
437 prognosis. *Am J Pathol* [Internet]. American Society for Investigative Pathology;
438 2001;158:987–96. Available from: [http://dx.doi.org/10.1016/S0002-9440\(10\)64045-X](http://dx.doi.org/10.1016/S0002-9440(10)64045-X)

439 54. Hagemann C, Blank JL. The ups and downs of MEK kinase interactions. *Cell Signal*.
440 2001;13:863–75.

441 55. Kim SY, Dunn IF, Firestein R, Gupta P, Wardwell L, Repich K, et al. CK1 ϵ is required for
442 breast cancers dependent on β -catenin activity. PLoS One. 2010;5.

443 56. Mahmoudi T, Li VSW, Ng SS, Taouatas N, Vries RGJ, Mohammed S, et al. The kinase
444 TNIK is an essential activator of Wnt target genes. EMBO J [Internet]. Nature Publishing
445 Group; 2009;28:3329–40. Available from: <http://dx.doi.org/10.1038/emboj.2009.285>

446 57. Ng SS, Mahmoudi T, Li VSW, Hatzis P, Boersema PJ, Mohammed S, et al. MAP3K1
447 functionally interacts with Axin1 in the canonical Wnt signalling pathway. Biol Chem.
448 2010;391:171–80.

449 58. Ding H, Takigawa I, Mamitsuka H, Zhu S. Similarity-based machine learning methods
450 for predicting drug-target interactions: A brief review. Brief Bioinform. 2013;15:734–47.

451 59. Zhang J, Huan J. Novel biological network features discovery for in silico
452 identification of drug targets. IHI' 10 - Proc 1st ACM Int Heal Informatics Symp.
453 2010;144–52.

454

Figures

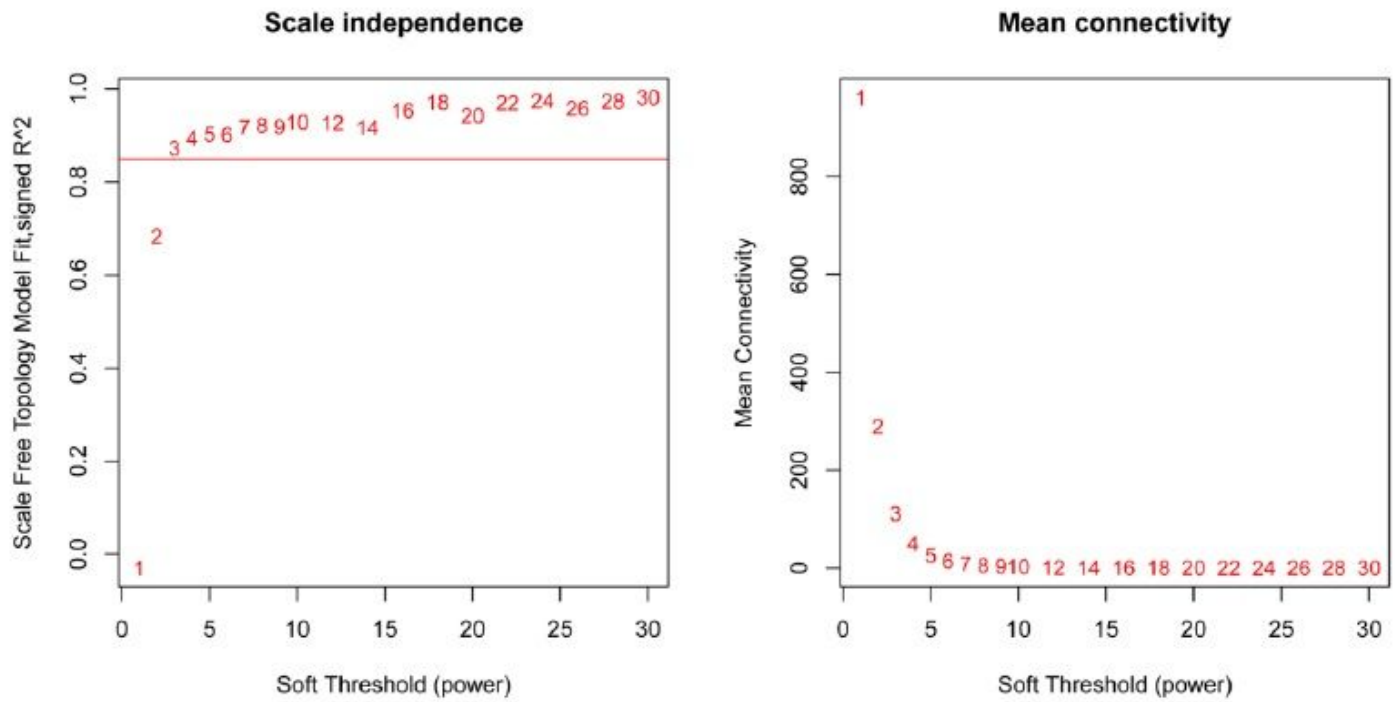


Figure 1

Determining the soft threshold power for the network topology. Analysis of the scale free fit index for various soft threshold powers (β) on the left. Analysis of the mean connectivity for various soft threshold powers in the right.

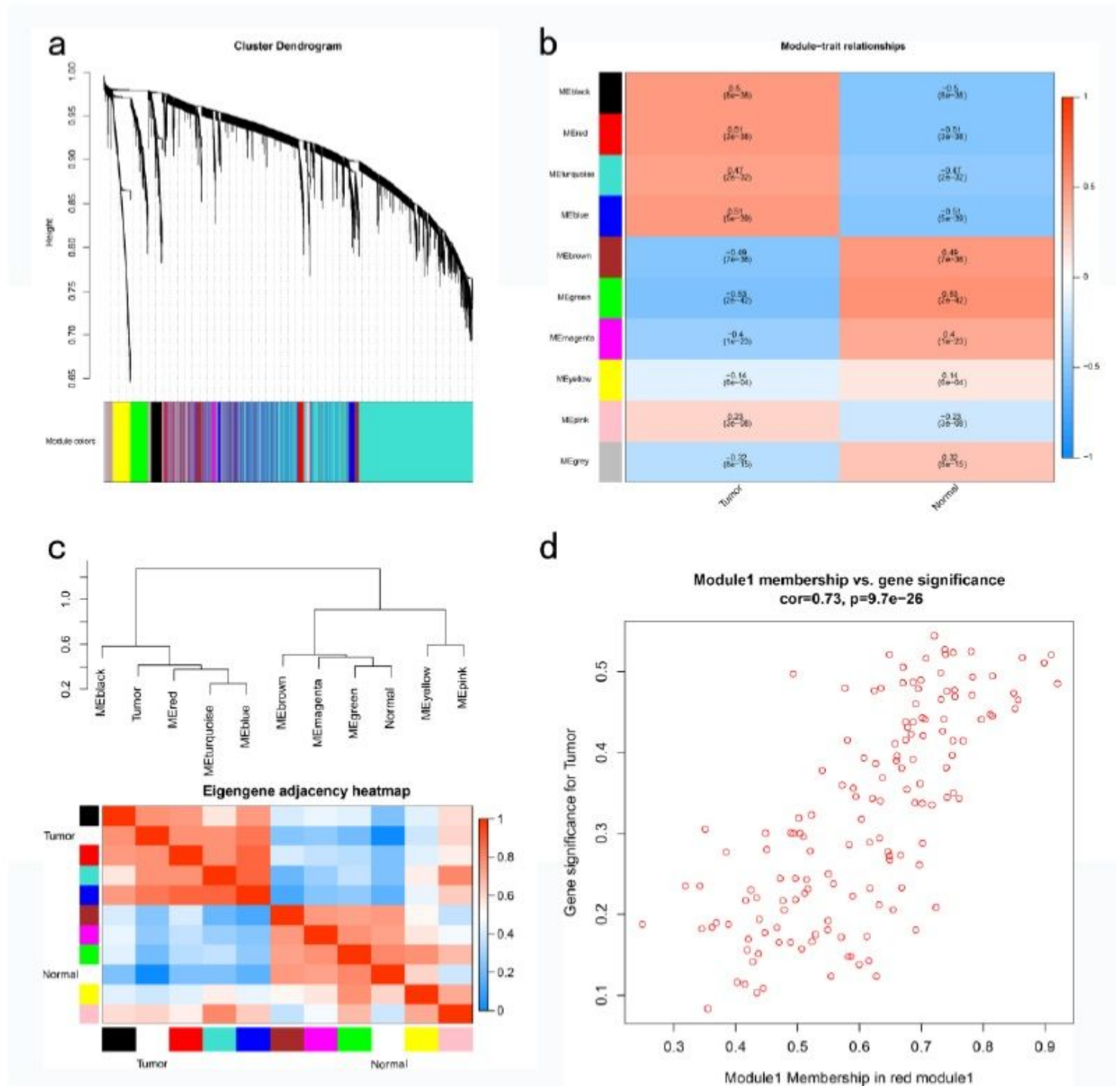


Figure 2

Gene enrichment and modules identified by Weighted gene coexpression network analysis (WGCNA). a Clustering dendrograms of screened genes. Different cluster modules were in different colors; b Heatmap of correlations between module eigengenes (ME) and thyroid cancer tissues. Each row represents a module eigengene, each column represents a thyroid cancer tissue and a normal thyroid tissue, and each cell contains the corresponding correlation and p-value. The matrices are color-coded by correlation

according to the color legend; c Dendrogram tree and adjacency heatmap of the eigengenes; d Scatterplot of the module membership and gene significance in the red module

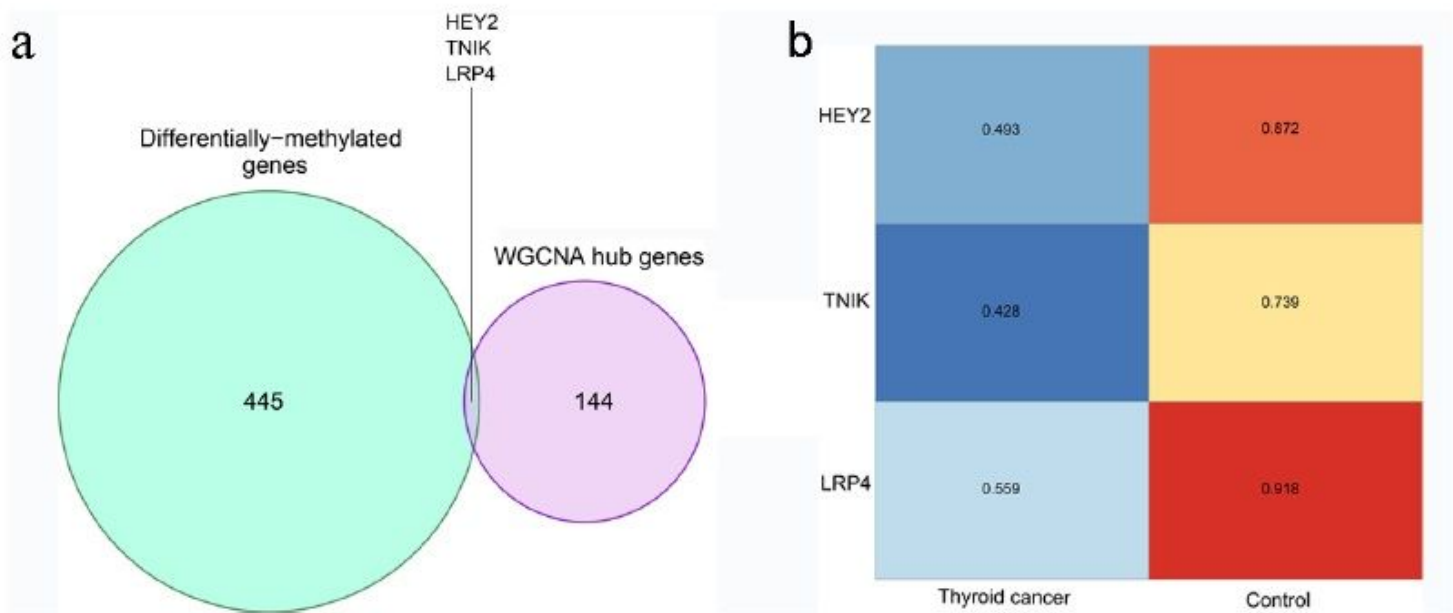


Figure 3

Screening out three genes from the intersection of DMGs and the red module. a Venn diagram between DMGs and hub genes in the red module showing the overlapping of three genes, HEY2, TNIK, LRP4; b Heatmap of DNA methylation in HEY2, TNIK, LRP4 between thyroid cancer tissues and normal thyroid tissue

TNIK

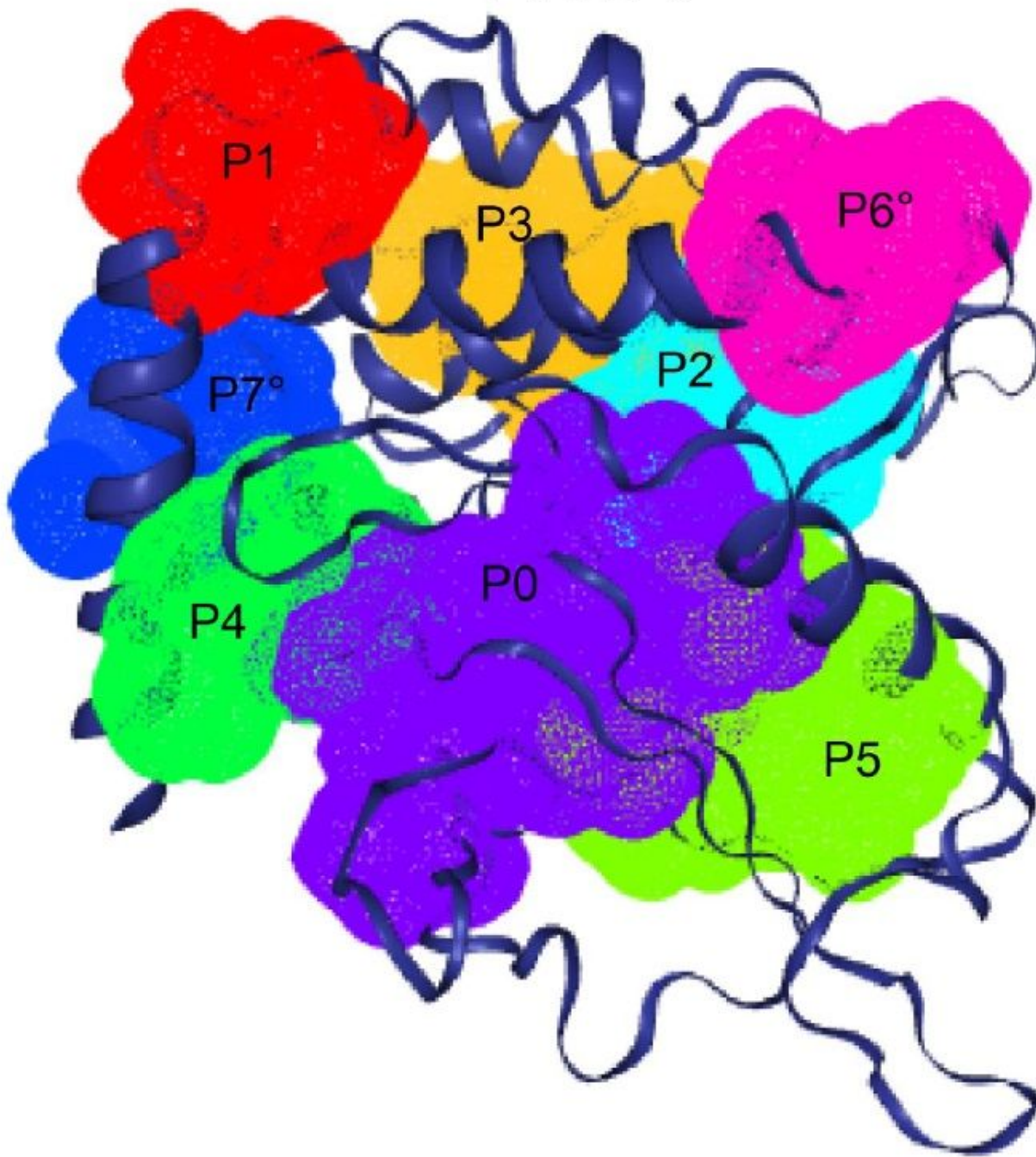


Figure 4

The protein pocket of TNIK. P0-P7 represent different protein pockets in TNIK

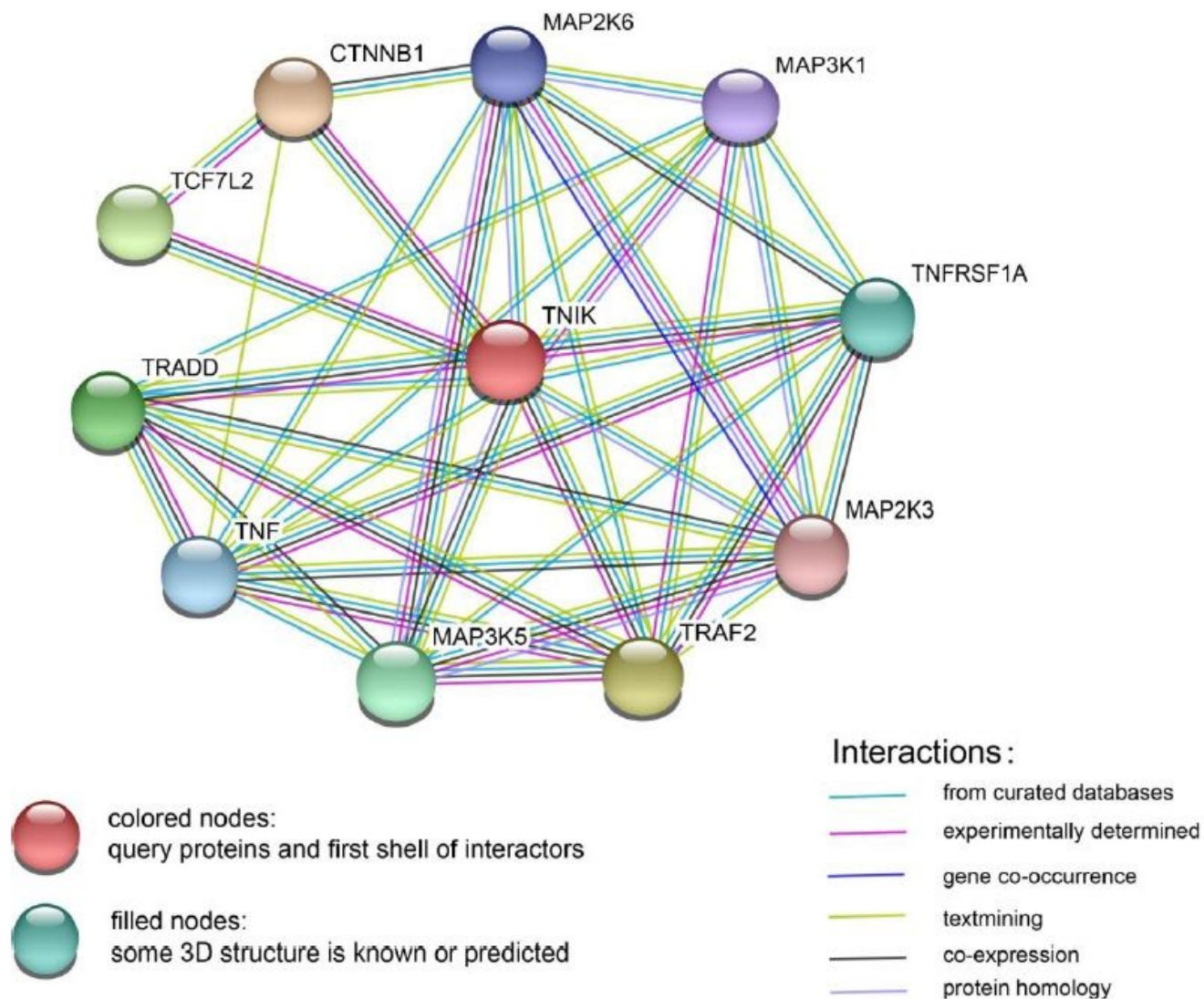


Figure 5

PPI network map for TNIK to identify targeted drug genes

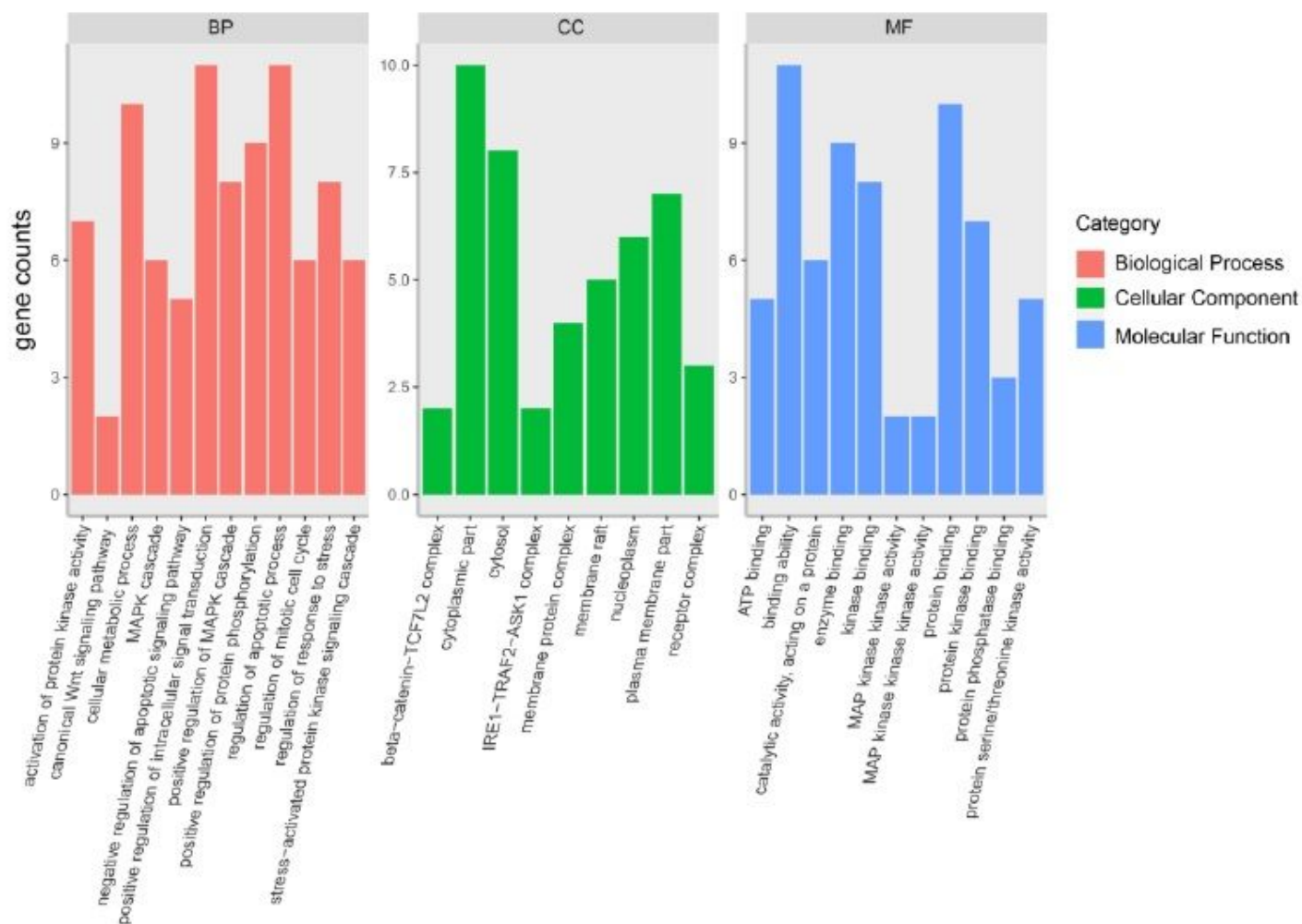


Figure 6

Gene Ontology (GO) enrichment of the genes in the PPI, including biological process (BP), molecular function (MF) and cellular component (CC)